P-ISSN 2586-9000
E-ISSN 2586-9027
Homepage : https://tci-thaijo.org/index.php/SciTechAsia
Science & Technology Asia
Vol.29 No.1 January - March 2024
Page: [226-238]
Original research article

The Failure of Repurposing Drug Therapies Based on *in vitro* and *in vivo* Studies: A Case Study of COVID-19

Teerachat Saeheng[1], Juntra Karbwang[2], Kesara Na-Bangchang[1,2,*]

[1]*Center of Excellence in pharmacology and molecular biology of malaria and cholangiocarcinoma, Chulabhorn International College of Medicine, Thammasat University, Pathum Thani 12120, Thailand*
[2]*Drug discovery and development center, Office of Advanced Sciences and Technology, Thammasat University, Pathum Thani 12120, Thailand*

Received 26 June 2023; Received in revised form 13 December 2023
Accepted 9 January 2024; Available online 31 March 2024

ABSTRACT

Ineffective selection of therapeutic drugs during an urgent situation leads to failure of COVID-19 treatment in large clinical trials, wasting time and money. We aimed to demonstrate the utility of physiologically-based pharmacokinetic (PBPK)/pharmacodynamic (PD) modeling to support the withdrawal of chloroquine (CQ) and ritonavir-boosted lopinavir (LPV/r) for COVID-19 treatment. The developed whole-body PBPK models were validated against clinical data. Model validation was performed using acceptable methods. The inhibitory effect was calculated to demonstrate drug efficacy. In different clinical trials, various regimens of CQ and LPV/r for COVID-19 treatment were used for simulation. The risk of cardiotoxicity following high-dose CQ administration was assessed. The effect of lung pH on drug concentrations in epithelial lining fluid (ELF) following a high CQ dose and LPV/r was evaluated. The whole-body PBPK models were successfully developed (AAFEs of 1.2-fold). The inhibitory effect (%E) of CQ following high-dose regimens in both ELF and bronchial epithelial cells (BEC) was lower than 2 and 1%, respectively. The corresponding values for the high dose of LPV/r were 40 and 2%, respectively. The risk of prolonged QTc in the population was higher than 20%. In addition, the %E of CQ was increased to 76% at pH 5.6 and decreased to 0.13% at pH 7.5. The change in pH in ELF did not influence LPV/r concentrations. PBPK/PD modeling supports the withdrawal of CQ and LPV/r for COVID-19 treatment as an effective tool for selecting therapeutic drug regimens in urgent situations.

Keywords: COVID-19; Chloroquine; Lopinavir/ritonavir/PBPK; SARs-COV2

***Corresponding author:** kesaratmu@yahoo.com **doi:** 10.14456/scitechasia.2024.17

1. Introduction

During the early COVID-19 pandemic, the rapid development of novel antiviral drugs to combat infection and meet urgent needs was limited. Repurposing approved drugs under advanced phases of clinical trials would be a preferable fast track. Ritonavir-boosted lopinavir (LPV/r) and chloroquine (CQ) were initially selected as repurposing drugs for COVID-19 therapy based on in vitro evidence. Still, they were finally withdrawn due to unsatisfactory treatment outcomes in large clinical trials [1]. In such an emergency, conducting large clinical trials may not be cost- or time-effective. Physiologically-based pharmacokinetic (PBPK) modelling is a pharmacokinetic model mimicking human physiology to explain drug disposition in the human body for dose-finding in various diseases [2]. PBPK/PD modelling has been successfully applied to select appropriate drug regimens and optimise doses in various diseases and conditions. It is also accepted by regulatory agencies as supplementary information for drug registration [3]. The present study aimed to demonstrate the utility of the PBPK and pharmacodynamic (PD) modelling as a tool to predict the clinical effectiveness of CQ and LPV/r for COVID-19 therapy.

2. Materials and Methods

2.1 Model construction

The whole-body PBPK models for LPV/r, CQ and rifampicin (used for model validation for the developed lung compartments) were constructed based on the information reported from previous studies [4, 5] using Simbiology® (version 5.8.2), a product of MATLAB® (version 2019a) (MathWorks, Natick, MA, USA). The lung compartments were divided into pulmonary circulation, lung-blood circulation, bronchial epithelial cells (BEC), and epithelial lining fluid (ELF). Model assumptions included a blood-flow limited model (except the lung compartment), immediate drug dissolution, absence of drug absorption in the stomach and large intestine, and absence of enterohepatic recirculation. The physicochemical and biochemical parameters of each drug are shown in Table 1. The goal of developing a PBPK model for rifampicin was to demonstrate the reliability of the novel simplified lung PBPK model in predicting additional substances or medications. The credibility of the model was achieved by accurately predicting the concentration of rifampicin in the BECs and the ELF.

Table 1. Physiologically-based pharma-cokinetic (PBPK) model input parameters for CQ, lopinavir, ritonavir, and rifampicin.

Parameter	Chloroquine	Lopinavir	Ritonavir	Rifampicin
Molecular weight (g/ mol)	319.9 [4]	628.81 [7]	721 [7]	823 [15]
Compound type	Diprotic base [4]	Neutral [7]	Dibasic base [7]	Ampholyte [15]
Log P	4.72 [4]	4.22 [7]	3.90 [7]	2.7 [15]
pKa	10.1, 8.38 [4]	NA	1.8, 2.8 [7]	1.7, 2.7 [15]
R_{bp} (B:P)	5 [4]	0.75 [7]	0.58 [7]	0.67 [16]
Fraction of unbound drug (fu)	0.55 [4]	0.01 [7]	0.015 [7]	0.34 [16]
Absorption rate (1/hours)	1.22 [4]	0.74 [7]	2.31 [11]	1.15 [17]
Apparent permeability ($P_{app, A-B}$) (10^{-6} cm/s)	16 [5]	0.0048 [8]	NA	640 [18]
Apparent permeability ($P_{app, B-A}$) (10^{-6} cm/s)	22 [5]	0.0320 [8]	NA	286 [18]
Solubility (mg/L)	NA	NA	500 [11]	NA
In vivo clearance (L/hours)	NA	NA	NA	10.3 [19]
Intrinsic clearance (µl/min/mg protein)				
CYP3A4	0.01 [6]	1.4 [8]	20.14 [13]	NA
CYP2D6	0.11 [6]	NA	0.93 [13]	NA
CYP2C8	0.08 [6]	NA	NA	NA
Renal clearance (L/hours)	4.6 [4]	NA	NA	1.5 [20]
Interaction-inhibition				
CYP3A4	NA	K_{inact}=6 (l/h), K_i=0·257 (mg/L) [10]	K_{inact}=19.8 (l/h), K_i=0.18 (mg/L) [14]	NA
Interaction-induction				
CYP3A4	NA	NA	Ind_{max}=2.45, Ind_{50}=13.9 (mg/L) [15]	NA

PBPK: physiologically-based pharmacokinetic, Log P: logarithm of octanol-water partition coefficient, pKa: negative decadal logarithm of acid dissociation constant, B:P: blood-to-plasma partition ratio, Kinact: inactivation rate of a given enzyme, Ki: inhibitor concentration yields half-maximal inhibition, Indmax: maximal fold induction, Ind50 concentration causing 50% maximal induction, Papp, A-B: apparent permeability from apical to basolateral, Papp, B-A: apparent permeability from basolateral to apical, NA: not applicable.

2.2 Model validation

The constructed models were validated using eight clinically published articles [6-13]. Model accuracy was evaluated based on absolute average-folding errors (AAFEs) (a comparison between predictive results and observed data) and a virtual predictive check (VPC). The accepted AAFEs value was < 2-fold [14]. The AAFEs equation is as follows:

$$AAFEs = 10^{\frac{\sum_{i=1}^{n}\left|\log\frac{\text{prediction}}{\text{observation}}\right|}{n}}, \qquad (2.1)$$

where n is the number of samples; predicted and observed PK/PD parameters are simulated and clinically observed data. The *AAFEs* value is reported as mean (±range).

2.3 Sensitivity analysis

Sensitivity analysis (a sensitivity coefficient) was performed to determine the effect of model parameters on the plasma drug concentrations following the 250 mg once-daily dose of CQ for 14 days. The model parameters for sensitivity analysis were absorption rate constant (K_a), fraction of unbound drug in plasma ($f_{u,p}$), and blood-to-plasma partition ratio ($R_{b:p}$). In addition, the fraction of unbound drug in tissue ($f_{u,t}$), pH in BEC and ELF, apparent permeability from apical-to-basolateral ($P_{app,\ A\text{-}to\text{-}B}$), and apparent permeability from basolateral-to-apical ($P_{app,\ B\text{-}to\text{-}A}$) were used for a sensitivity analysis following a single 600 mg dose of rifampicin and twice-daily dose of 400/100 mg LPV/r for 14 days. Each model parameter was varied by ±20% from its original value. The selected model parameters are crucial factors that significantly affect the prediction of unbound drug concentrations in the designated tissues, which are necessary for determining the treatment's effectiveness. One hundred virtual populations were simulated with the fixed values of other model parameters (constant values). The equation for sensitivity analysis is as follows:

$$\text{sensitivity coefficient} = \frac{\nabla Y}{\nabla X}, \qquad (2.2)$$

where %Y and %X are the percent changes of the AUC312:336h and model parameter, respectively. A schematic workflow is shown in Fig. 1.

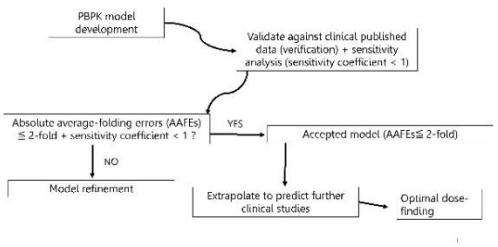

Fig. 1. A schematic workflow of model simulation and analysis.

2.4 PBPK-PD model

A Pharmacodynamic (PD) model (Emax model) was constructed to assess the inhibitory effect of each study drug on SARs-COV-2 according to the following equation:

$$E = \frac{E_{\max} * A_{u,lung\ tissue}}{EC_{50,u} + A_{u,lung\ tissue}}, \qquad (2.3)$$

where E is inhibitory effect; Emax is maximal inhibition; $EC_{50,u}$ is the half-maximal effective concentration (unbound drug); and $A_{u,\ lung\ tissue}$ is the amount of unbound drug in BEC (lung tissue) (mol/L or M). The $E_{\max}$ and $EC_{50,u}$ of LPV/r were 0.89 and 21.7 µM, respectively [15]. The corresponding values for CQ were 0.9 and 64.7 µM, respectively [15, 16]. The EC_{50} values were selected to calculate the EC_{90} using the Hill function and then multiplied by the fraction of unbound drug [the fraction of unbound drug (f_u) refers to a particular value determined through a dose-response curve test conducted under specific conditions]. The f_u for CQ and lopinavir (LPV/r) was assumed to be 1 due to low protein concentration in the experimental environment compared with blood/plasma or tissue. The inhibitory effect (%E), and amount of unbound drug in BEC and ELF are presented as mean (±95% confidence interval (CI)). The %E total is the inhibitory effect of a combination of LPV/r and chloroquine.

2.5 Dose simulations based on clinical trials

One hundred virtual populations (50 males and 50 females, aged 18-60 years, weighing 60 kg, fasting state) with eight clinical scenarios were simulated as follows:

Chloroquine: multiple oral doses of 300 mg base CQ given twice daily for (i) 7 days in patients with mild COVID-19 (scenario-I) (average negative PCR on day 16) [17]; (ii) 10 days for patients with mild COVID-19 (average negative PCR on day 14) (scenario-II) [18]; (iii) 14 days in patients with moderate COVID-19 (average negative PCR on day 14) (scenario-III); and (iv) 600 mg base CQ given twice daily for 14 days in patients with severe COVID-19 (average negative PCR on day 13) (scenario-IV) [19].

Lopinavir/ritonavir: multiple oral doses of 400/100 mg LPV/r given twice daily for (i) 7 days in patients with mild/moderate COVID-19 (average negative PCR on day 21) (scenario-V) [20]; (ii) 14 days in patients with mild/moderate COVID-19 (average negative PCR on day 14) (scenario-VI) [21]; (iii) 10 days in patients with mild/moderate COVID-19 (median hospital discharge on day 11) (scenario-VII) [22]; and (iv) loading doses of 800/200 mg LPV/r for two doses, followed by 600/150 mg twice daily on day 2 for 9 days in patients with mild/moderate COVID-19 (scenario-VIII) [23].

2.6 Effect of ELF pH on drug concentrations

The pH in normal ELF in healthy airways is acidic (5.5 to 7.5) [24], which may influence the degree of ionization of CQ and LPV/r, resulting in the change in the amount of unbound drug in ELF. The pH in the ELF was set as 6.9. The effects of ELF pH on the amount of unbound CQ and LPV/r were simulated at four pH values, i.e., 5.6, 6.5, 6.9, and 7.5.

2.7 Assessment of risk of cardiac arrythmia based on clinical simulations

Since CQ is associated with the risk of cardiac arrythmia with prolongation of corrected QT (QTc) interval [25], the effects of various dosage regimens of CQ on QTc were evaluated following the previously published PK-QTc relationship [25]. The equation to describe the relationship between CQ concentration and QTc is shown below:

$$QT_{prediction} = QT_{baseline} + 0.006CQ_{concentration}. \quad (2.4)$$

A published article was used to validate the risk of QTc prolongation. One hundred virtual populations (50 males and 50 females, aged 18-60 years, weighing 40-70 kg) were simulated. Results are reported as the percentage of predicted peak QTc following 600 mg base of CQ given twice daily for 14 days [25] and 300 mg base of CQ given twice daily for 14 days in COVID-19 patients with severe symptoms.

3. Results and Discussion

3.1 Model verification

The *AAFEs* are summarized in Table 2, and the VPCs are shown in Figs. 2-4. The *AAFEs* for all regimens was 1.2 [6-13]. The *AAFEs* for ritonavir, chloroquine, LPV/r and rifampicin in plasma were 1.29 (1.18-1.59) [8], 1.21 (1.15-1.26) [11,12], 1.18 (1.08-1.27) [6,7] and 1.16 (1.13-1.18) [11-13], respectively. The *AAFEs* of ELF (rifampicin and LPV/r) and BEC (rifampicin) were 1.09 (1.02-1.17) [4,11] and 1.19 [11], respectively. For chloroquine, sensitivity coefficient values for K_a, f_u and $R_{b:p}$ were +0.13, -0.90 and +0.06, respectively. The sensitivity coefficient of rifampicin ELF for fu,t, pH in BEC, pH in ELF, $P_{app,\ A\text{-}to\text{-}B}$ and $P_{app\ B\text{-}to\text{-}A}$ were -0.53, -0.16, -0.05, -0.07, and -0.60, respectively. The corresponding values of rifampicin for BEC were +0.56, -0.18, -0.08, -0.10 and -0.61, respectively. *AAFEs* of 1.5-fold and sensitivity coefficients of <1 indicated (within 2-fold) the model's reliability and applicability for simulations of further scenarios.

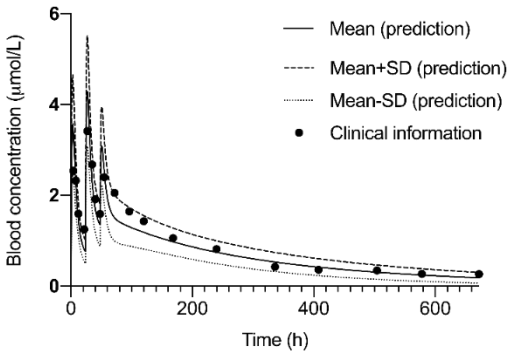

Fig. 2. A comparison of loading dose of 600 mg on day 1, followed by 600 mg on day 2, and followed by 300 mg on day 3 in healthy volunteer between prediction and observation [1].

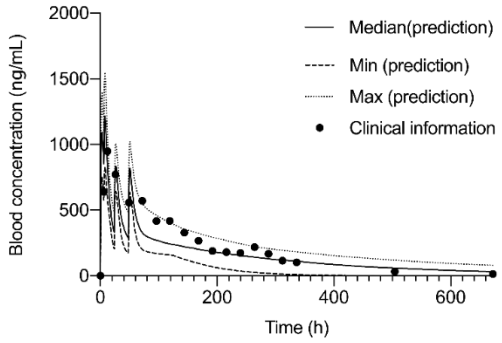

Fig. 3. A comparison of multiple doses of 600 mg on day 1, followed by 600 mg on day 2, and followed by 300 mg on day 3 in Thai healthy subjects between prediction and observation [2].

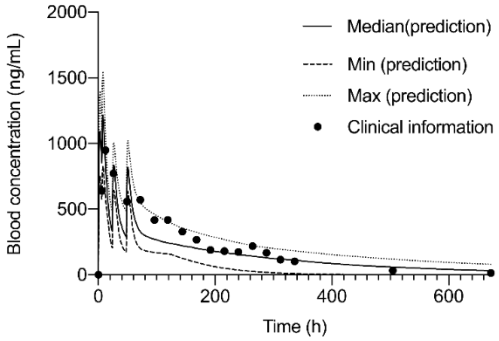

Fig. 4. A comparison of a single dose of 300 mg CQ administration in healthy volunteer between prediction and observation [3].

Table 2. Model validation based on absolute-average folding errors (AAFEs).

Clinical study	PK parameter	Predicted value	Observed value	Predicted value /Observed value
Chloroquine				
A single dose of 600 mg administration in healthy subjects [9]	$AUC_{0\text{-}7days}$ (µM*h)	88.79 (69.31-118.78)	90.0 (48.90-212.3)	0.98
	C_{max} (µM)	2.84 (2.15-3.48)	1.80 (1.30-5.20)	1.58
	V_d/F (L)	7,825 (4,898-10,057)	8672 (2,593-32,503)	0.90
	CL/F (L/h)	10.56 (6.11-17.48)	11.30 (5.70-20.30)	0.93
	$T_{1/2}$ (days)	22.21 (8.83-43.98)	23.30 (10.2-54.60)	0.95
	AAFEs			1.15
Loading dose of 600 mg administration on day 1, followed by 600 mg on day 2, and followed by 300 mg on day 3 in healthy volunteers [9]	$AUC_{0\text{–}28days}$ (µM*h)	488.26 (251.11-992.98)	636.3 (394.2-1010.9)	0.77
	C_{max} (µM)	4.09 (2.44-7.70)	3.4 (1.4-5.6)	1.20
	V_d/F (L)	5,876 (1,770-12,260)	3,721 (1,248-20,516)	1.58
	CL/F (L/h)	9.8 (4.7-19.2)	9.5 (5.4-20.6)	1.03
	$T_{1/2}$ (days)	16.47 (4.76-57)	13.2 (4-44)	1.25
	AAFEs			1.26
Multiple doses of 600 mg administration on day 1, followed by 600 mg on day 2, followed by 300 mg on day 3 in Thai healthy subjects [10]	$AUC_{0\text{–}28days}$ (µg*h/mL)	112.32 (58.50-163.07)	122 (103-182)	0.92
	C_{max} (ng/mL)	1,220 (830-1,550)	838 (658-1,587)	1.45
	$T_{1/2}$ (hours)	144.76	150	0.96
	AAFEs			1.26
Chloroquine	AAFE			1.21
Ritonavir				
Multiple doses of 200 mg of ritonavir given every 12 hours for 2 weeks [8]	$AUC_{24h,day16}$ (µg*h/mL)	64.11	43.80	1.46
	C_{max} (µg/mL)	5.02	4.5	1.11
	C_{min} (µg/mL)	0.64	0.60	1.06
	AAFEs			1.20
Multiple doses of 300 mg of ritonavir given every 12 hours for 2 weeks [8]	$AUC_{24h,day16}$ (µg*h/mL)	107.04	60.70	1.76
	C_{max} (µg/mL)	7.99	6.50	1.23

	C_{min} (μg/mL)	1.30	0.70	1.86
	AAFEs			1.59
Multiple doses of 400 mg of ritonavir given every 12 hours for 2 weeks [8]	$AUC_{24h,day16}$ (μg*h/mL)	139.71	114.20	1.22
	C_{max} (μg/mL)	10.39	11.70	0.88
	C_{min} (μg/mL)	1.74	1.10	1.58
	AAFEs			1.30
Multiple doses of 500 mg of ritonavir given every 12 hours for 2 weeks [8]	$AUC_{24h,day16}$ (μg*h/mL)	191.25	170.30	1.12
	C_{max} (μg/mL)	13.22	14.20	0.93
	C_{min} (μg/mL)	3.13	2.30	1.36
	AAFEs			1.18
Ritonavir	AAFEs			1.30
Lopinavir				
Multiple doses of lopinavir/ritonavir (400/100 mg) given twice daily for 3 weeks [7]	$AUC_{24h,day21}$ (μg*h/mL)	217.97	185.2	1.17
	C_{max} (μg/mL)	10.52	9.81	1.07
	C_{trough} (μg/mL)	7.08	7.13	0.99
	AAFEs			1.08
Multiple doses of lopinavir/ritonavir (800/200 mg) given once daily for 3 weeks [7]	$AUC_{24h,day21}$ (μg*h/mL)	221.09	164.90	1.34
	C_{max} (μg/mL)	12.14	10.94	1.11
	C_{trough} (μg/mL)	5.05	3.62	1.39
	AAFEs			1.27
Multiple doses of lopinavir/ritonavir (400/100 mg) given twice daily [6]	Plasma-concentration (μg/mL)	7.95	8.10	0.98
	Epithelial lining fluid concentration (μg/mL)	17.47	14.4	1.21
	AAFEs			1.11
Lopinavir	AAFEs			1.17
Rifampicin				
Single dose of 450 mg [11]	AUC_{0-24h} (μg*h/mL)	62.33	44	1.42
	C_{max} (μg/mL)	5.70	6.60	0.86
	Clearance (L/hours)	8.62	8.70	0.99
	AAFEs			1.18
Single dose of 600 mg [12]	AUC_{0-24h} (μg*h/mL)	85.92	76.95	1.12
	C_{max} (μg/mL)	7.95	9.85	0.81
	Clearance (L/hours)	8.67	8.25	1.05
	AAFEs			1.13
Single dose of 600 mg [13]	Bronchial mucosa concentration (μg/mL)	9.29	7.90	1.17
	Epithelial lining fluid concentration ((μg/mL)	4.71	5.5	0.86
	AAFEs			1.17
Rifampicin	AAFEs			1.16
All drugs	AAFEs			1.20

3.2 Chloroquine

Scenario-I: The $A_{u,CQ}$ in BEC and ELF were 253 (246-261) (Fig. 5) and 1,800 (1,747-1,852) nM (Fig. 5), respectively. The %*E* for BEC and ELF were 0.035 (0.035-0.036) and 0.740 (0.710-0.770)%, respectively.

Scenario-II: The $A_{u,CQ}$ in BEC and ELF were 329 (321-337) (Fig. 5) and 2,338 (2,281-2,395) nM (Fig. 5), respectively. The %*E* for BEC and ELF were 0.045 (0.043-0.046) and 0.950 (0.920-0.980)%, respectively.

Scenario-III: The $A_{u,CQ}$ in BEC and ELF were 345 (334-356) (Fig. 5) and 2,453 (2,376-2,530) nM (Fig. 6), respectively. The %*E* for BEC and ELF were 0.053 (0.051-0.055)% and 1.120 (1.080-1.150)%, respectively.

Scenario-IV: The $A_{u,CQ}$ in BEC and ELF were 729 (710-747) (Fig. 5) and 5,174 (5,042-5,307) nM (Fig. 6), respectively. The %*E* for BEC and ELF were 0.102 (0.098-0.105) and 2.120 (2.050-2.190)%, respectively.

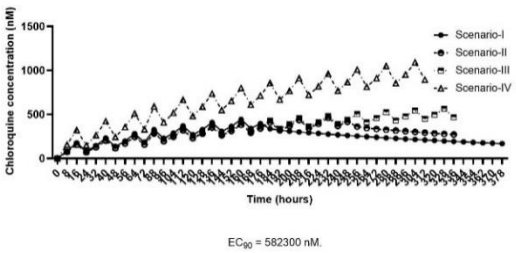

Fig. 5. Comparisons of the amount of CQ in bronchial epithelial cells (BEC) with different scenarios (I-IV) and the cut-off level.

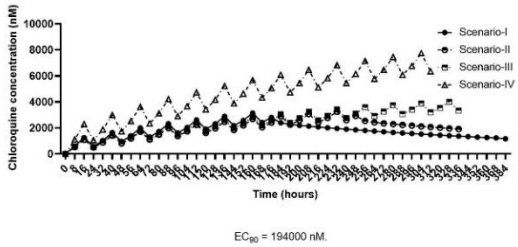

Fig. 6. Comparisons of the amount of CQ in extracellular lining fluid (ELF) with different scenarios (I-IV) and the cut-off level.

CQ is, therefore, ineffective against SARs-COV-2 either through the blockage of viral entry (ELF) or viral replication (BEC). The PBPK-PD modelling results support the decision to withdraw CQ for COVID-19 treatment since the inhibitory effect (%E) of the drug for both BEC and ELF in all scenarios was lower than 2% and 1%, respectively. As SARs-CoV-2 particles most likely enter the human body through the human epithelial airway or bronchial mucosa, the ELF is likely to be first exposed to the viral particles before entering the lungs. Such a low CQ concentration (<EC90) in ELF (Fig. 6) is inadequate to prevent viral entry. Besides this, the inhibitory effect of CQ on viral entry blockage (ELF) was low. This is explained by the weak binding affinity (-3.3 to -5.9 kcal/mol) of CQ to angiotensin-converting enzyme 2 (ACE-2) [26], a crucial receptor for a severe acute respiratory syndrome coronavirus 2 (SARs-CoV-2) infection. As the binding affinity of SARs-CoV-2 (wild type) to ACE-2 is about 10-fold higher (up to -49.94 kcal/mol) [27], chloroquine, therefore, cannot compete with SARs-COV-2 virus for the binding site and thus cannot block viral entry. Furthermore, the drug also cannot prevent viral replication in the lung epithelial cells when the viral particles infect BEC since the concentrations in the BEC is about 500-600-fold lower than the EC90 (Fig. 5). Cathepsin L (CTSL) is an endosomal protease crucial for the viral endocytosis and glycoprotein processing of SARs-CoV-2 within the cell. This mechanism is essential for the subsequent viral replication. The fusion processes between SARs-COV2 and lysosomes may be inhibited by CQ binding to the CTSL receptor. CQ may impede the release of genomic materials of SARs-COV2 into the BEC by blocking the CTSL receptor. Results of the docking simulation also suggest that this endosomal protease is a poor target for CQ (high binding affinity of -5.4 kcal/mol) [28]. In addition, results of the in vitro study in Calu-3 cell lines also showed the weak inhibitory effect of CQ on SARs-CoV-2 (IC50 up to 64.7 µM) [15]. Since CQ is ineffective for both the blockage of viral entry and replication, the drug is likely to be ineffective for both prevention and treatment of COVID-19.

The findings of this study confirm that administering multiple doses of 300 mg base CQ twice daily for 7 to 14 days (scenarios I to III) does not effectively reduce the time it takes to achieve PCR-negative results or shorten the duration of hospitalization. Additionally, this treatment does not effectively prevent the progression of the disease. Overall, extending the administration period of CQ at 300 mg twice a day from 7 to 14 days (scenarios I-III) did not substantially reduce the time required for patients with mild-to-moderate symptoms to become PCR-negative. There was no significant difference in the time for individuals taking CQ and those receiving supportive care to test negative for PCR. This corresponds with the simulated decrease in the percentage of effectiveness (%*E*) in BEC for scenarios I to III, which is less than 1%. This suggests that the inhibitory effects of CQ on SARs-COV2 infection are not successful in reducing hospitalization time.

Furthermore, the simulation showed that an accumulation of CQ in BEC (situation I-III) was inefficient in inhibiting viral replication processes. This is because the amount of CQ in BEC in scenarios I, II, and III was 2,300, 1,769, and 1,687 times lower than the EC90, respectively. Administering higher doses (600 mg twice daily, intravenously) to patients with severe symptoms did not affect the time required for the PCR test to provide a negative result. The value amounted to less

than 0.1% of the %*E*, with the amount of CQ being 800 times lower than the EC90 in BEC. The accurate estimation of the CQ and %E in BEC and ELF (the target sites where the drug acts) demonstrated that the projected outcomes were consistent with the observed clinical results in all scenarios. Hence, PBPK models are advantageous for facilitating decision-making and addressing drug utilization during urgent public needs before conducting clinical trials, particularly when repurposing drugs.

3.3 Lopinavir/ritonavir

Scenario-V: The $A_{u,LPV/r}$ in BEC and ELF were 532 (492-571) (Fig. 7) and 263 (243-283) nM (Fig. 8), respectively. The %*E* for BEC and ELF were 0.470 (0.440-0.510) and 11.06 (10.54-11.58)%, respectively.

Scenario-VI: The $A_{u,LPV/r}$ in BEC and ELF were 1524 (1,407-1,640) (Fig. 7) and 754 (697-811) nM (Fig. 7), respectively. The %*E* for BEC and ELF were 1.37 (1.26-1.47) and 30.57 (29.14-32.0)%, respectively.

Scenario-VII: The $A_{u,LPV/r}$ in BEC and ELF were 1486 (1378-1594) (Fig. 7) and 735 (682-789) nM (Fig. 8), respectively. The %*E* for BEC and ELF were 1.34 (1.24-1.43) and 30.09 (28.84-31.33)%, respectively.

Scenario-VIII: The $A_{u,LPV/r}$ in BEC and ELF were 2658 (2449-2867) (Fig. 7) and 1,315 (1,212-1,419) nM (Fig. 8), respectively. The %*E* for BEC and ELF were 2.35 (2.18-2.53) and 41.47 (39.96-42.98)%, respectively.

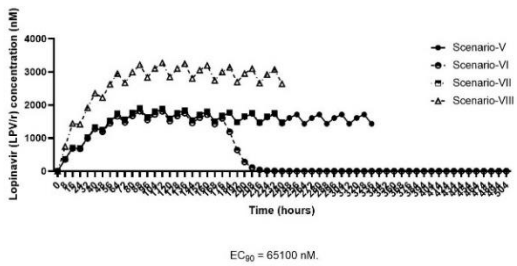

Fig. 7. Comparisons of the amount of lopinavir (scenario-V-VIII) in bronchial epithelial cells (BEC) and the cut-off level.

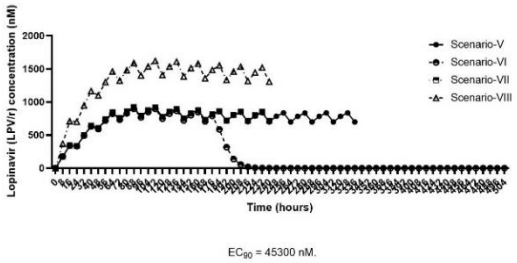

Fig. 8. Comparisons of the amount of lopinavir (scenario-V-VIII) in extracellular lining fluid (ELF) and the cut-off level.

The simulated results also support the decision to withdraw LPV/r for COVID-19 treatment since the %*E* of LPV/r in ELF was lower than 20% (Scenario-V). Therefore, any dose regimens of LPV/r are inadequate to provide sufficient concentrations of LPV in plasma, ELF, and BEC to inhibit viral entry or replication. The ineffective treatment efficacy of LPV/r in Scenario-V could be explained by the delay and inadequate treatment duration (termination of the drug after the 9-day course of treatment) before confirmation of a negative COVID-19 test (16 days). Premature termination of drug administration would lead to insufficient maintenance of drug concentrations and inhibitory effects. Furthermore, the %*E* of LPV/r in BEC was as low as < 2% and would be inadequate to inhibit viral replication in lung epithelial cells. Although the full standard course of LPV/r (400/100 mg LPV/r given twice daily for 10 to 14 days) was given (Scenario-VI-VII), LPV concentrations at the target sites (ELF and BEC) were still inadequate. This regimen provided LPV concentrations 60- and 128-fold lower than the EC90 values for SARs-CoV-2 inhibition in the BEC and ELF (Figs. 6-7), respectively. The standard regimen of LPV/r was ineffective for patients with mild to moderate COVID-19 (%*E* of LPV/r for the BEC and ELF was lower than 1.5% and 30 %). Even with an increased dose of LPV/r up to 800/200 mg twice daily for two doses on day 1, followed by 600/150 mg twice daily for up to 10 days (Scenario-VIII), despite the increase in %*E* for both BEC and ELF, the inhibitory

effects were still too low (2 and 40%, respectively). They would be ineffective for both prevention and treatment of COVID-19.

Transmembrane serine protease-2 (TMPRSS-2) has been reported as a crucial receptor for SARs-CoV-2 entry [29]. During the early outbreak of COVID-19, LPV/r was proposed as an effective inhibitor of TMPRSS-2 and ACE-2 with moderate affinity (binding scores of -7.261 and -7.890, respectively) [29], and a potential drug candidate for a COVID-19 treatment. The trough plasma concentration of LPV at steady-state following the standard dose regimen was 13.6 mg/L [17], while the EC50 of LPV for inhibition of SARs-CoV-2 was 13.64 mg/L (21.7 µM, Calu-3 cell lines) [15]. Corrected unbound LPV/r level in plasma was only 0.136 mg/L (f_u=0.01), while unbounded EC50 was 13.64 mg/L (low protein binding in the in vitro studies) [15]. However, the plasma concentration-time profiles could not represent the drug concentration at target sites e.g., BECs and ELF. In addition to TMPRSS-2 and ACE-2, LPV is a potent inhibitor of SARs-COV-2 replication via 3CLpro with a binding affinity of -8 kcal/mol [30].

Altogether, results suggest that the screening methods for repurposing drugs based on information from the in vitro studies and molecular studies are not reliable enough to conclude the efficacy of LPV/r or any other repurposing drugs for treating new emerging diseases. PBPK/PD modeling, on the other hand, is an effective tool for selecting a potential drug candidate to meet the requirement during an urgent circumstance.

3.4 Effect of ELF pH on CQ and LPV/r

Chloroquine: For pH 5.6, the $A_{u,CQ}$ in BEC and ELF were 638 (615-660) and 1,649,912 (1,591,718-1,708,106) nM, respectively. The %*E* for BEC and ELF were 0.097 (0.093-0.10) and 76.19 (75.88-76.50)%, respectively. For pH 6.5, the $A_{u,CQ}$ in BEC and ELF were 660 (636-683) and 29,543 (28,488-30,599) nM, respectively. The %*E* for BEC and ELF were 0.101 (0.098-0.105) and 11.63 (11.27-11.99)%, respectively. For pH 7.5, the $A_{u,CQ}$ in BEC and ELF were 639 (618-660) and 286 (276-295) nM, respectively. The %*E* for BEC and ELF were 0.098 (0.095-0.10) and 0.132 (0.128-0.137)%, respectively. The Au CQ values are shown in Fig. 5.

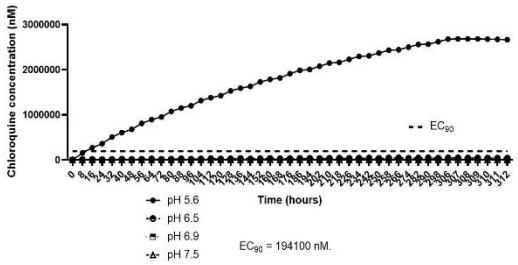

Fig. 5. Comparison of the effect of different extracellular lining fluid (ELF) pH values on the amount of CQ in ELF with cut-off level.

LPV/r: For pH 5.6, the $A_{u,LPV/r}$ in BEC and ELF were 2,481 (2,278-2,684) and 1,228 (1,128-1,329) nM, respectively. The %*E* for BEC and ELF were 2.20 (2.03-2.38) and 40.07 (38.56-41.58)%, respectively. For pH 6.5, $A_{u,LPV/r}$ in BEC and ELF were 2,737 (2,711-2,762) and 1,355 (1,230-1,479) nM, respectively. The %*E* for BEC and ELF were 2.41 (2.20-2.63) and 41.43 (39.77-43.10)%, respectively. For pH 7.5, $A_{u \text{ and } LPV/r}$ in BEC and ELF were 2,625 (2,430-2,820) and 1,299 (1,203-1,396) nM, respectively. The %*E* for BEC and ELF were 2.33 (2.17-2.49) and 41.37 (39.90-42.84)%, respectively. Generally, changes in ELF pH dramatically affected CQ concentration in ELF but not in BEC. The ELF pH of 5.6 was reported in patients with bacterial pneumonia [24]. In acidic conditions, chloroquine's %*E* (ELF) to prevent viral entry appears adequate to prevent SARs-CoV-2 infection to lung epithelial cells. Nonetheless, patients with pneumonia are in a critical situation, and CQ is unlikely to provide effective therapy. Instead, these patients require treatment with immunomodulators. Unlike chloroquine, the changes of ELF pH had no influence on LPV/r concentrations in both ELF and BEC.

3.5 Cardiological toxicities

The percentage of QTc prolongation (over 500 milliseconds) following 600 mg base of CQ given twice daily for 14 days with an average patient body weight of 70 kg was 21%. This result is in agreement with those from a reported clinical study [19]. The corresponding value with an average patient body weight of 40 kg was 47%.

The percentage of QTc prolongation following 300 mg base of CQ given twice daily for 14 days with an average patient body weight of 40 kg was 5%. There was no change in QTc (0%) with an average patient body weight of 70 kg.

CQ is cardiotoxic, inducing QTc prolongation even when administered in a short duration [31]. At a low dose (300 mg base twice daily for 7 to 14 days) in Scenario-I to III, there was no evidence of QTc prolongation (< 500 milliseconds) in patients with an average body weight (70 kg). Surprisingly, after a low dose of 300 mg CQ administered twice daily, there were no reports or assessments of QTc prolongations in those clinical trials [17, 18]. Nevertheless, additional unfavorable occurrences associated with gastrointestinal symptoms, such as nausea, vomiting, and abdominal discomfort, were documented. However, an increased risk of QTc prolongation was found in patients with an average body weight of 40 kg without any benefit regarding COVID-19 treatment. At a higher dose (Scenario-IV), the estimated percentage of patients experiencing QTc prolongation was 21% in those with an average body weight of 70 kg, which closely aligned with the findings of a clinical investigation (18.9%) [19].

Furthermore, Becker and colleagues documented that 24% (17 out of 70) of patients who were administered 600 mg of CQ twice daily developed QTc prolongation (> 500 ms) within 48 hours after administration [31]. Furthermore, 11% (4 out of 36) of patients experienced QTc prolongation when the dosage was reduced to 450 mg [19]. Significantly, the likelihood of QTc prolongation is contingent upon the dosage administered, which is directly linked to the levels of CQ in the blood. A positive correlation was seen between the levels of CQ in the blood and the prolonging of QTc [25]. Caution should be exercised when administering CQ at high doses to patients with low body weight, as indicated in this study, due to the increased risk of QTc prolongation in such individuals. The study findings suggest that administering a high CQ dosage may not be suitable for individuals, as it raises the risk of QTc prolongation, especially in those with a body weight of 70 kg or less. Clinical investigations have determined that a dosage of 300 mg administered twice daily is considered safe, as no significant adverse effects have been recorded, especially concerning QTc prolongation. It may be because those patients' average body weight was over 40 kg. Nevertheless, those weighing 40 kg, as indicated by the simulation, are susceptible to a potential 5% risk of QTc prolongation. For LPV/r, gastrointestinal adverse events are generally the most commonly reported adverse effects of LPV/r. LPV/r also has been shown to increase QTc and PR prolongation risk in COVID-19 patients [32]. At high doses, increases in alanine-amino-transferase of ≥ 3 times the upper limit and ≥ 5 times the upper normal limit were reported in 24 and 12% of COVID-19 cases, respectively [23]. Furthermore, as a potent CYP3A inhibitor, LPV/r may lead to drug-drug interactions when administered with other drugs. Combination therapy of LPV/r and CQ is not recommended due to ineffective treatment and an increased risk of QTc prolongation.

4. Conclusion

In summary, the results of this study support the decision to withdraw CQ and LPV/r for COVID-19 treatment. The application of PBPK/PD modelling could assist in selecting appropriate drug regimens while maximizing efficacy and minimizing

risks prior to confirmation in clinical trials to save time and resources.

Acknowledgements

This work was supported by Thammasat University (Postdoctoral Fellowship, Center of Excellence in Pharmacology, and Molecular Biology of Malaria, and Cholangiocarcinoma), Thailand Science Research and Innovation Fundamental Fund, and the National Research Council of Thailand under the Research Team Promotion Grant. All funders have no roles for publication. We thank Dr. Marco Siccardi and Dr. Rajith Kumar Reddy Rajoli, department of Molecular and Clinical Pharmacology, University of Liverpool, for their support and advice

References

[1] World Health Organization (WHO). WHO discontinues hydroxychloroquine and lopinavir/ritonavir treatment arms for COVID-19., 2020. Retrieved from: https://www.who.int/news/item/04-07-2020-who-discontinues-hydroxychloro-quine-and-lopinavir-ritonavir-treatment-arms-for-covid-19. Accessed: 20 October 2021.

[2] Perazzolo S., Zhu, L., Lin W., et al. Systems and clinical pharmacology of COVID-19 therapeutic candidates: a clinical and translational medicine perspective. J. Pharm. Sci. 2020;110(3): 1002-17.

[3] Zhao P. Report from the EMA workshop on qualification and reporting of physiologically based pharmacokinetic (PBPK) modeling and simulation. CPT: Pharmacometrics Syst Pharmacol. 2016;2: 71-2.

[4] Saeheng T., Na-Bangchang K., Siccardi M., et al. Physiologically-based pharmacokinetic modelling for optimal dosage prediction of quinine co-administered with ritonavir-boosted lopinavir. Clin Pharmacol Ther. 2019;5: 1209-20.

[5] Siccardi M., Rajoli R.K.R., Dickinson L., et al. In silico simulation of interaction between rifampicin and boosted darunavir., 2015. Retrieved from: http://www.croiconference.org/sessions/silico-simulation-interaction-between-rifampicin-and-boosted-darunavir. Accessed 20 October 2021.

[6] Atzori C., Villani P., Regazzi M., et al. Detection of intrapulmonary concentration of lopinavir in an HIV-infected patient. AIDs. 2003;11: 1710-11.

[7] Eron J.J., Feinberg J., Kressler, H.A., et al. Once-daily dose versus twice-daily lopinavir-ritonavir in antiretroviral-naïve HIV-positive patients: a 48-week randomized clinical trial. J. Infect Dis. 2004;2: 265-72.

[8] Hsu A., Granneman G.R., Witt G. et al. Multiple-dose pharmacokinetics of ritonavir in human immunodeficiency virus-infected subjects. Antimicrob Agents Chemother 1997;5: 898-905.

[9] Mzayek F., Deng H., Mather F.J., et al. Randomized dose-ranging controlled trial of AQ-13, a candidate antimalarial, and chloroquine in healthy volunteer. PLoS Clin Trials. 2007;2: e6.

[10] Na-Bangchang K., Limpaibul L., Thanavibul A. et al. The pharmacokinetics of chloroquine in healthy Thai Subjects and patients with Plasmodium vivax malaria. Br J Clin 1994;3: 278-81.

[11] Rafiq S., Iqbal, T., Jamil A., Khan, F.H. Pharmacokinetic studies of rifampicin in healthy volunteers and tuberculosis patients. Int J Agric Biol. 2010;12: 391-5.

[12] Rasool MF., Khalid S., Majeed A., et al. Development and evaluation of physiologically based pharmacokinetic drug-disease models for predicting rifampicin exposure in tuberculosis and cirrhosis population. Pharmaceutics. 2019;11: 578.

[13] Ziglam H.M., Baldwin D.R., Daniels I., Andrew, J.M., Finch, R.G. Rifampicin concentrations in bronchial mucosa,

epithelial lining fluid, alveolar macrophages, and serum following a single 600 mg oral dose in patients undergoing fibre-optic bronchoscopy. J Antimicrob Chemother. 2002;6: 1011-5.

[14] Saeheng T., Na-Bangchang K, Karbwang J. Utility of physiologically-based pharmacokinetic (PBPK) modeling in oncology drug development and its accuracy: a systematic review. Eur J Clin Pharmacol. 2018;74(1): 1365-76.

[15] Ko M., Jeon S., Ryu W.S., Kim S. Comparative analysis of antiviral efficacy of FDA-approved drugs against SARs-CoV-2 in human lung cells. J Med Virol. 2020;3: 1403-8.

[16] Hoffmann M., Mosbauer K., Hofmann-Winkler H., et al. Chloroquine does not inhibit infection of human lung cells with SARs-CoV-2. Nat. 2020;7826: 588-90.

[17] Gao G., Wang A., Wang S., F. et al. Brief report: retrospective evaluation on the efficacy of lopinavir/ritonavir and chloroquine to treat non-severe COVID-19 patients., J Acquir Immune Defic Syndr. 2020;2: 239-43.

[18] Huang M., Tang T., Pang P., et al. Treating COVID-19 with chloroquine. Nat Rev Mol Cell Biol. 2020;12(4): 322-5.

[19] Borba MGS., Val FFA., Sampaio VS., et al. Effect of high vs low doses of chloroquine diphosphate as adjunctive therapy for patients hospitalized with severe acute respiratory syndrome coronavirus 2 (SARs-CoV-2) Infection: A randomized clinical trial. JAMA Netw Open. 2020;4: 3208857.

[20] Kim JW., Kim EJ., Kwon HH., et al. Lopinavir-ritonavir versus hydroxychloroquine for viral clearance and clinical improvement in patients with mild to moderate coronavirus disease 2019. Korean J Intern Med. 2021;36 (Suppl 1): S253-63.

[21] Huang M., Li M., Xiao F., et al. Preliminary evidence from a multicenter prospectively observational study of the safety and efficacy of chloroquine for the treatment of COVID-19. Natl Sci Rev. 2020;9: 1428-36.

[22] Recovery collaborative group. Lopinavir-ritonavir in patients admitted to hospital with COVID-19 (RECOVERY): a randomised, controlled, open-label, platform trial. Lancet. 2020;10259: 1345-52.

[23] Karolyi M., Omid S., Pawelka E., et al. High dose lopinavir/ritonavir doses not lead to sufficient plasma levels to inhibit SARs-CoV-2 in hospitalized patients with COVID-19. Front Pharmacol. 2021;12: 704767.

[24] Zajac M., Dreano E., Edwards A., Planelles G., Sermet-Gaudelus I. Airway surface liquid pH regulation in Airway epithelium current understanding and gaps in knowledge. Int J Mol Sci. 2021;7: 3384.

[25] Ursing J., Rombo L., Eksborg S., Larson, L., et al. High-Dose Chloroquine for Uncomplicated Plasmodium falciparum Malaria Is Well Tolerated and Causes Similar QT Interval Prolongation as Standard-Dose Chloroquine in Children. Antimicrob Agents Chemother. 2020;3: e01846-19.

[26] Badraoui R., Adnan M., Bardakci F., Alreshidi MM. Chloroquine and hydroxychloroquine interact differently with ACE2 domains reported to bind with the coronavirus spike protein: mediation by ACE2 polymorphism. Molecules. 2021;3: 673.

[27] Ali F., Kasry A., and Amin M. The new SARs-CoV-2 stran shows a stronger binding affinity to ACE-2 due to N501Y mutant. Med Drug Discov. 2021; 10: 100086.

[28] Yamamoto N., Matsuyama S., Hoshino T., Yamamoto, N. Nelfinavir inhibits replication of severe acute respiratory syndrome coronavirus 2 in vitro. bioRxiv. 2020.

[29] Baby K., Maity S., Mehta CH., Suresh A., Nayak UY., Nayak Y. SARs-CoV-2 entry inhibitors by dual targeting TMPRSS2 and ACE2: an in silico drug repurposing study. Eur J Pharmacol. 2021; 896: 173922.

[30] Chen YW., Yiu CPB., Wong KY. Prediction of SARs-CoV-2 (2019-nCoV) 3C-like protease (3CL-pro) structure: virtual screening reveals velpatasvir, ledipavir, and other drug repurposing candidates. F1000Res. 2020;9: 129.

[31] Becker ML., Snijders D., van Gemeren CW., Kingma HJ., van Lelyveld SFL., and Giezen T. QTc prolongation in COVID-19 patients using chloroquine. Cardiovasc Toxicol. 2021;4: 314-21.

[32] Haghjoo M., Golipra R., Kheirkhah J., et al. Effect of COVID-19 medications on corrected QT interval and induction of torsade de pointes: results of a multicenter national survey. Int J Clin Pract. 2021;7: e14182.